Aquifer Vulnerability Index Model for Vulnerability Assessment: A Case Study of Irewolede Estate in Ilorin, North-Central Nigeria

Abubakar, H. O.[1] | Adebisi, W. A.[2]✉ |Folorunso, I. O.[1] | Adeoye, T. O.[1] | Olatunji, S.[1] | Odangbe, C. O.[1]

1. Department of Geophysics, Faculty of Physical Sciences, University of Ilorin, Ilorin, Nigeria.
2. Department of Physical and Chemical Sciences, Faculty of Science, Federal University of Health Sciences, Ila-Orangun, Osun State, Nigeria.

Corresponding Author E-mail: warith.adebisi@fuhsi.edu.ng

Abstract

An Electrical Resistivity Survey was conducted in the Irewolede Estate, located within the Ilorin Metropolis, with the objective of evaluating the susceptibility of the weathered geological layer to contamination. A total of 16 Vertical Electrical Sounding data points were collected and analyzed to delineate the geo-electric stratigraphy, assess hydrogeological implications, and evaluate aquifer vulnerability. The investigation identified five distinct geo-electric layers, including a shallow aquiferous layer exhibiting resistivity values ranging from 28.2 to 876 Ωm and thickness measurements ranging from 4.94 to 71.5 m. The spatial distribution of the Aquifer Vulnerability Index (AVI) indicated that the majority of the region exhibited moderate vulnerability, succeeded by areas of low vulnerability. Regions characterized by high and extremely low vulnerability were noted as small, isolated patches. In order to avert aquifer contamination, the study advocates for thorough geophysical and geotechnical investigations prior to the establishment of future landfills in the region. The findings of this research provide significant insights into the subsurface geological conditions and aquifer vulnerability, which can guide decisions regarding the appropriate placement of groundwater resources and the siting of landfills. By implementing proactive strategies, the potential risk of aquifer contamination can be effectively mitigated, thereby ensuring a sustainable and secure water supply for the community.

Keywords: Irewolede Estate, Vertical Electrical Sounding, Stratigraphy, Aquifer Vulnerability Index.

1. Introduction

Groundwater plays a vital role in housing estates, serving as a crucial component of sustainable urban planning, livelihoods, economic development, and ecosystems (Amanambu et al., 2020; Pointet, 2022). As the world's population grows exponentially, the demand for clean water and sanitation also increases, making groundwater a vital resource for meeting these needs. Groundwater remains the primary source of freshwater, often considered a more feasible supply of potable water than surface water sources. It significantly contributes to the residents health, well-being, and livelihoods and removes certain impurities while moving through soils and subterranean formations (Udosen et al., 2024). Groundwater provides a reliable source of clean drinking water for residents, supports proper wastewater management and sanitation systems, sustaining green spaces, gardens, and recreational areas. Additionally, it can serve as a major supply for firefighting purposes.

Groundwater protection is a critical component of sustainable housing estate development and management. However, the resources within housing estates face numerous threats, including contamination, over-extraction, and land subsidence, which can jeopardize both the quality and quantity of groundwater, rendering it vulnerable to pollution. Groundwater vulnerability refers to the degree to which an aquifer is susceptible to contamination, specifically whether the subsurface characteristics can either prevent or facilitate the transport of contaminants into

the aquifer (Jain, 2023; Machiwal et al., 2018; Sethi & Di Molfetta, 2019). Groundwater flow velocity is a key control on vulnerability and it depends on two factors: the hydraulic conductivity of protective covering layers and the depth of the water-table. Furthermore, it is affected by various factors including the geological properties of the region, hydrological processes, and human activities on the surface (Taghavi et al., 2022). Therefore, knowing the groundwater vulnerability will be helpful for effective water resource management and protection.

There are several mechanisms through which pollutants enter the groundwater system, leading to pollution. The principal sources of pollution owing to the rapid development of the world population, urbanization, industrialization, and agricultural production, industrial and agricultural waste, and inadequate waste management (Li et al., 2021). Chemicals, heavy metals, and solvents produced by industrial activities often harm the environment through soil water percolation, which infiltrates into groundwater (Briffa et al., 2020). Similarly, agricultural methods such as fertilizer, pesticides, and herbicides, can lead to the contamination of groundwater resources (Baweja et al., 2020; Singh et al., 2022). These chemicals are extensively introduced to battle pests and diseases, seeping into groundwater and poisoning drinking watersheds.

Aquifers are underground layers of porous rock or sediment that hold and transmit water, or bodies of saturated rock or geological formations through which water can easily flow (permeability) into wells and streams (Salako & Adepelumi, 2018). These rock formations are highly susceptible to contamination from both natural and human-induced factors. Classifying sensitive aquifers is critical to preventing contamination and ensuring an adequate supply of safe and clean groundwater for human consumption and other necessary uses. This process involves conducting hydrogeological studies, mapping vulnerability zones, and implementing appropriate management strategies. Monitoring programs can help detect the presence of contaminants and understand their sources and transport mechanisms. Additionally, the implementation of proper waste management practices, regulation of industrial activities, and adoption of

sustainable agricultural practices can minimize the risk of groundwater pollution.

The Aquifer Vulnerability Index (AVI) model is a widely used tool for assessing the vulnerability of aquifers to contamination, playing a crucial role in water resource management and protection (Ekanem, 2022). The AVI model provides a comprehensive and systematic approach to assess the susceptibility of aquifers to various pollutants, allowing for effective decision-making, mitigation strategies, and sustainable management practices. The AVI model incorporates several key indicators and parameters that influence the vulnerability of aquifers, such as geological characteristics, hydrogeological conditions, land use practices, and sources of pollutants (Jain, 2023). By considering these factors, the model calculates a vulnerability index that indicates the likelihood of contamination reaching the groundwater and the potential impact it may have.

Residents of the Irewolede housing estate frequently express concerns about the unpleasant taste and dark coloration of the water when fetched into transparent containers. Before the establishment of the area for housing estates, the soil had previously hosted a large waste dumpsite (landfill). The rising demand for water, combined with inadequate waste management and poor land use practices, may all have contributed to exacerbating the risk of aquifer contamination. Therefore, there is a need for a thorough AVI assessment to identify vulnerable areas, prioritize protection efforts, and inform sustainable water resource management strategies within the estates.

In earlier research, Obiora and Ibuot (2020) conducted a geophysical study to evaluate aquifer vulnerability at the University of Nigeria, Nsukka, Enugu State, Nigeria. Using electrical soundings and resistivity tomography, they estimated hydraulic conductivity and resistance values, which ranged from 0.0434 to 0.4890 m/day and 38.37 to 1005.84 day^{-1} respectively. The AVI revealed that the study area has low to high vulnerability, with moderate vulnerability being the most prevalent. This research aimed to identify aquifer protective zones and potential locations for groundwater exploration and management. However, the study's localized focus on a university campus

may limit its applicability to areas with different hydrological settings and environmental conditions, such as those with a history of significant waste disposal or agricultural activities.

This study aims to evaluate the vulnerability of the weathered aquifer at Irewolede Estate in Ilorin, Kwara State, Nigeria, by applying hydrogeological assessment methods, including the AVI model. Specifically, the study will determine the depth and thickness of the geoelectric layers that protect the aquifer, estimate geohydraulic parameters to assess the vulnerability index of the aquifer protective layers, develop a vulnerability map, highlighting areas with high, moderate, and low susceptibility to contamination, and propose an efficient and cost-effective groundwater management strategy based on the results of the vulnerability assessment.

2. Location and Geological Setting

The study area is the Irewolede Housing estate, located in Ilorin, Kwara State, Nigeria (Figure 1). The region experiences total annual rainfall ranging from 800 mm to 1200 mm in the northwest and 1000 mm to 1500 mm in the southeast. The estate has a mean annual temperature ranging between 30^0C and 35^0C, with an average relative humidity of 60%. Major landmarks surrounding the Irewolede housing estate include the Emir of Ilorin's Palace to the north, Asa Water Lake to the south, and the Oko-Erin community to the west.

Geologically, the Ilorin region is a distinctly intricate area situated within the Southwestern Basement Complex of Nigeria. This region is characterized by the presence of the Migmatite–Gneiss–Quartzite complex which constitutes about 75% of all rocks in the area, which dates from the Precambrian to Cambrian periods and are intruded by various suites of granitic formations, including porphyritic granite, medium/coarse-grained biotite granite, hornblende granite, granodiorite, and granite gneiss. Collectively, these are referred to as the Older granitoid, which are attributed to the Pan-African orogeny in the northern, central, and southwestern sectors. Additionally, younger metasedimentary formations, which constitute about 20% of the rocks in the study area and are likely of Pan-African origin, are found beneath the southeastern portion of the study area (Balogun, 2019).

3. Materials and Methods

The materials utilized in this investigation comprise a compass clinometer used for field navigation. The compass performs basic tasks such as orientation, while the built-in clinometer allows geologists to measure the dip of rock beds, the height of geological and geographical features, and various angles. Additionally, GPS devices are employed to acquire coordinate and elevation data. Four metallic stakes or rods identified as electrodes, employed for the injection of electrical current into the subsurface and the measurement of the potential difference therein. Insulated cabling interconnects the electrodes to the resistivity meter. The terrameter SAS 300C system, manufactured by ABEM instruments, is employed for the quantification of the earth's resistance. IPI2WIN least-squares iterative inversion software is applied for one-dimensional resistivity inversion, while a Microsoft Excel workbook is employed for data handling. Finally, the Surfer Software program is used to generate contour maps.
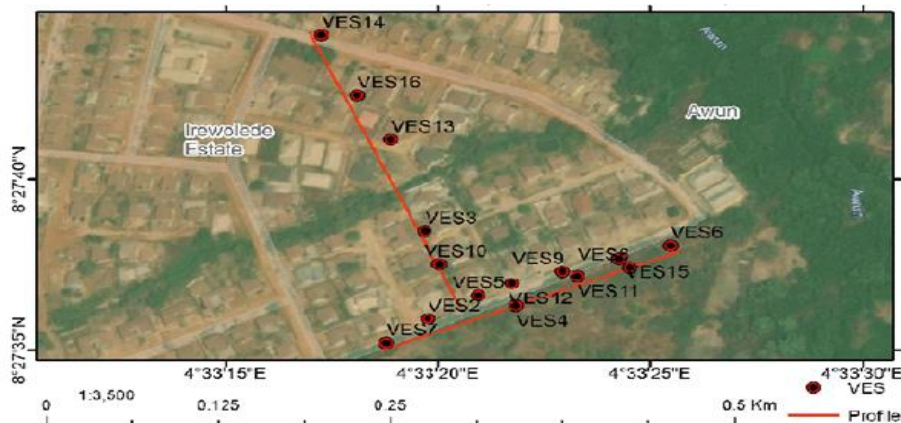

Figure 1. Google earth map showing the study area and layout for the acquisition of VES data.

Sixteen Vertical Electrical Soundings (VES) employing the Schlumberger electrode configuration were used in this survey (Figure 2). This technique is widely used in resistivity studies and involves arranging a series of four electrodes in a straight line, with the current electrodes (A and B) at the ends and the potential electrodes (M and N) in between. An electrical current is injected into the ground through the pair of current electrodes, and the voltage drop is measured at increasing distances from the current source. The maximum separations of the current electrodes (AB) ranged logarithmically from 1 m to 200 m. This spread was considered long enough to evaluate the protective sandy-clayey layer and the shallow weathered aquifer to a depth of about 35 m. The apparent resistance R_a of the penetrated geologic material was read from the display unit of the resistivity meter. The values of resistivity are calculated by multiplying the apparent resistance recorded from the resistivity meter by the corresponding geometric factor of the electrode array configuration given by:

$$\rho_a = KR_a \tag{1}$$

In which K is the geometric factor, given by:

$$K = 2\pi\left[\left(\frac{1}{r_1} - \frac{1}{r_2}\right) - \left(\frac{1}{r_3} - \frac{1}{r_4}\right)\right]^{-1} \tag{2}$$

A review of field data for errors and inconsistencies was conducted initially. The apparent resistivity values obtained were plotted against half the current electrode spacing (AB/2) on a bi-logarithmic graph sheet characterized by a dynamic range for smoothening and correction of outliers that were viewed as noise. The smoothened resistivity curve was electronically inverted and modelled to true resistivity using the IPI2WIN software program based on the Newton algorithm to solve the inverse problem. This software generates VES curves, which also provide primary parameters, including true resistivity, thickness, and depth. An error value was generated after the inversion to help have an understanding of the level of noise present in the field data.

The ability of groundwater to flow through the subsurface, known as hydraulic conductance (K), is influenced by the layer resistivity of a geologic unit. Since subsurface rocks are porous and fractured, hydraulic conductivity measures how easily water moves through these spaces. Accurately estimating hydraulic conductivity is crucial for identifying areas with high aquifer potential within weathered and fractured zones. To achieve this, a predictive model developed by Tijani et al. (2021) was used to derive hydraulic conductivity values from resistivity data, specifically tailored for regions with similar geological characteristics.

$$K = 0.5019\rho^{-1.054} \tag{3}$$

Where K is the hydraulic conductivity and ρ is geoelectric layer resistivity

The AVI constitutes a methodology that assesses vulnerability based on the hydraulic resistance encountered by vertical water flow traversing the overlying strata (Stempvoort et al., 1993). The calculation of the AVI is predicated upon two critical parameters: the thickness (h) of the protective layers and the estimated hydraulic conductivity (K). The hydraulic resistance (C) is derived from these parameters and is articulated as:

$$\sum_{i=1}^{n} \frac{h_i}{K_i} \tag{4}$$

where K_i is the hydraulic conductivity and h_i is the thickness

Table 1 shows the relationship between hydraulic resistance (C) and the AVI model used in determining the vulnerability level.
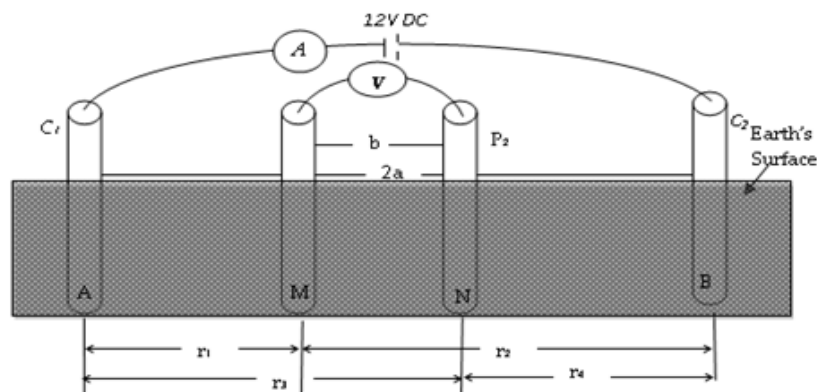

Figure 2. Vertical electrical sounding Schlumberger Array Mode (Olatunji & Musa, 2014).

Table 1. Relationship between aquifer vulnerability index (AVI) and hydraulic resistance.

Hydraulic Resistance	Log C	Vulnerability (AVI)
0 - 10	<1	Extremely high
10 -100	1 – 2	High
100 -1000	2 – 3	Moderate
1000 - 10000	3 – 4	Low
>10000	>4	Extremely low

4. Results and Discussions

Table 2 presents results of the inversion of field electrical resistivity data from the first eight (8) VES points, showing the formation resitivities, thicknesses, and depths. The modelled geo-electric layers within the study area range from three to five. The resistivity curve types identified within the study area include A, H, HA, HK, and KH. The inequality of the curve types is of the order A>HA>KH>H>HK. Figure 3 is a bar graph that shows the proportion of the resistivity curve types across the study area. The inferred geoelectric lithology of the geoelectric layers is topsoil, sandy clay, laterites, weathered basement, and fresh basement. In this study, the weathered basement is considered to be the aquiferous layer, and the topsoil, sandy clay, and laterites are considered the aquifer cover or protective layer. The thickness and resistivity of the protective layer are calculated as the sum of the thicknesses of each unit and the average of the resistivities, respectively.

Table 2. Result of Inversion of field electrical resistivity data for the first eight (8) VES.

| VES	LAT	LONG	No. of Layers	ρ (Ωm)	H	d	Curve Type	Inferred lithology
VES1	8.46233	4.55242	3	72.9	5.31	14.46	A	Topsoil
				438	9.15			Weathered B.
				1348				Fresh Basement.
VES2	8.46008	4.55567	4	98.3	1.09	16.64	HK	Topsoil
				590	5.58			Laterites
				213	9.97			Weathered B.
				4226				Fresh Basement.
VES3	8.4603	4.55556	4	188	0.531	20.241	HA	Topsoil
				66.7	5.91			Laterites
				768	13.8			Weathered B.
				1151				Fresh Basement.
VES4	8.46008	4.55607	3	50.3	0.952	10.542	A	Topsoil
				876	9.59			Weathered B
				3121				Fresh Basement.
VES5	8.46011	4.55599	3	164	1	9.44	A	Topsoil
				700	8.44			Weathered B
				1653				Fresh Basement.
VES6	8.46057	4.55708	4	334	1.95	18.68	KH	Topsoil
				832	3.13			Laterites
				256	13.6			Weathered B
				2444				Fresh Basement.
VES7	8.45978	4.55522	4	103	0.701	34.801	HA	Topsoil
				26.3	4.8			Laterites
				145	29.3			Weathered B.
				1313				Fresh Basement.
VES8	8.46039	4.55681	3	174	1.17	6.11	A	Topsoil
				325	4.94			Weathered B.
				3545				Fresh Basement.
LAT = Latittude, LONG=Longittude, ρ = Apparent Resistiivity, h = Layer Thickness, d = Layer Depth								
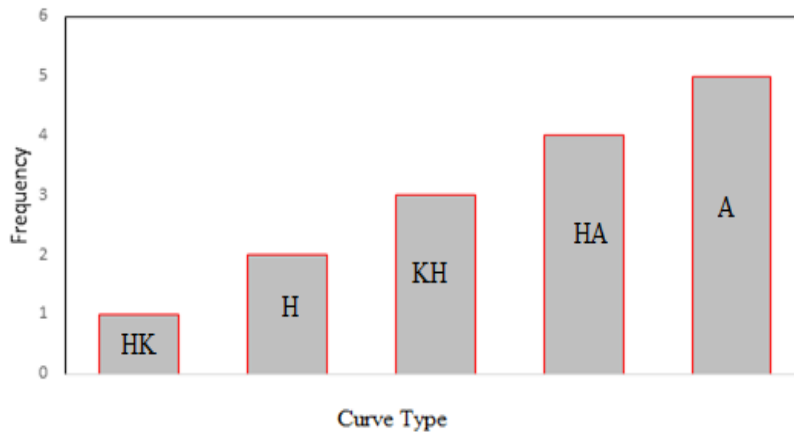
Figure 3. Bar graph showing the distribution of curve types across the study area.

Generally, the resistivity of layer 1 ranges from 14 to 334 Ωm, and its thickness ranges from 0.5 to 5.31 m, which is inferred to be the topsoil layer. The second layer, believed to be laterite, shows resistivity values ranging from 9.59 to 832 Ωm and a thickness between 1.0 and 8.35 m. The third layer, believed to be clayey sand, has a resistivity of 2779 and a thickness of 0.413 m. The fourth layer is described as the shallow aquiferous layer in the area, with resistivity values between 28.2 and 876 Ωm and thickness values between 4.94 and 71.5 m. The fifth layer with relatively high average resistivity values of 716 to 5343 Ωm, is considered to be the fresh, unweathered basement, with the depth to the top of this layer varying between 6.11 and 74.51 m.

4-1. Thickness of Overlying Layers
Figure 4 shows a contour map illustrating the distribution of the cumulative overlying thicknesses. It shows high thickness in the north-central flank, which decreases toward the southeastern region. This area of high thickness corresponds to more protectiveness for the underlying aquifer material, as contaminants are likely to travel longer distances through the vadose zone.

4-2. Thickness of the Aquiferous Layer
Figure 5 illustrates the stratigraphic thickness of the aquiferous layer, revealing that regions in the southeastern flank exhibit elevated values and consequently possess relatively enhanced groundwater potential. The predominant measurement of aquifer thickness indicates that the aquiferous layer is typically shallower (less than 50 m). Such aquifers are likely to exhibit a diminished capacity for groundwater storage. Moreover, these regions may be characterized by the presence of dense or impermeable geological formations.
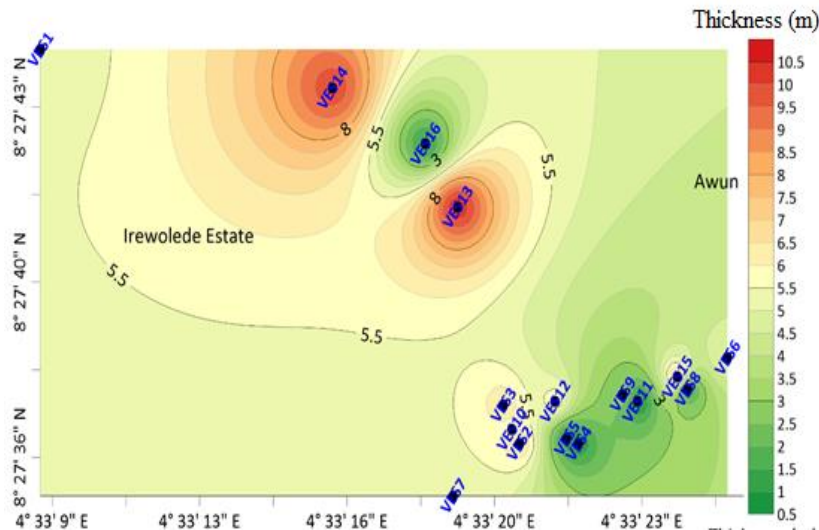

Figure 4. Contour map showing the distribution of thickness of the overlying layers.
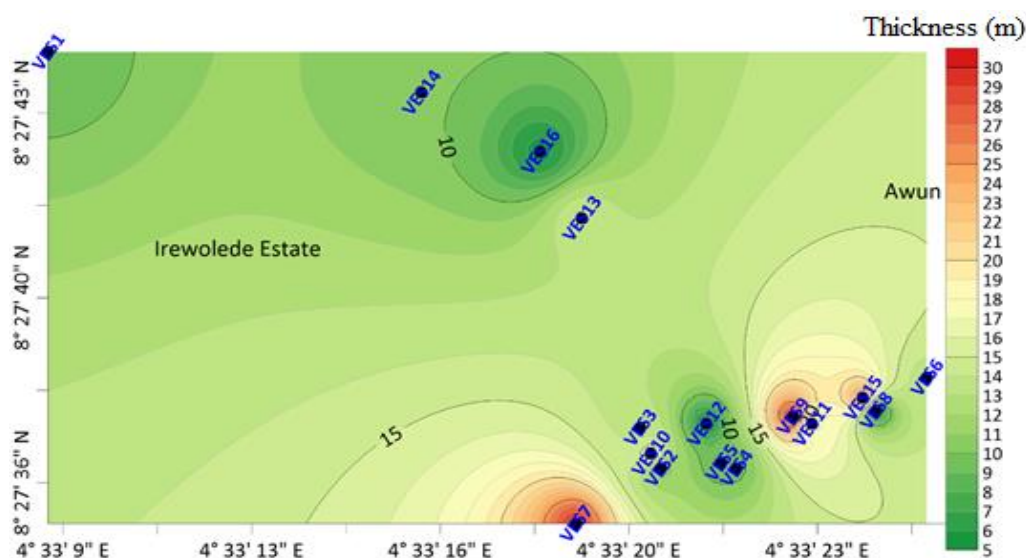
Figure 5. Contour map showing the distribution of thickness of the aquiferous layers.

4-3. Hydraulic Conductivity

Table 3 shows computed hydraulic conductivity (K) for the study area, which ranges from 2.3×10^{-4} to 3.2×10^{-2} mday^{-1}. The estimated hydraulic conductivity (K) was subsequently contoured (Figure 6), revealing a spatial variability characterized by a decrease in K in the eastern and western regions. This pattern suggests an enhanced protective capacity of the underlying aquifer. Conversely, regions with higher K values are at a greater risk of groundwater contamination.

Table 3. Estimated geohydraulic parameters.

ID	LONG	LAT	H cover	H aquifer	K	C	Log C	AVI rating
VES1	4.55242	8.46233	5.31	9.15	5.4×10^{-3}	972.28	2.99	Moderate
VES2	4.55567	8.46008	6.67	9.97	1.0×10^{-3}	6269.61	3.80	Low
VES3	4.55556	8.46030	6.441	13.8	3.0×10^{-3}	2123.27	3.33	Low
VES4	4.55607	8.46008	0.952	9.59	8.0×10^{-3}	117.89	2.07	Moderate
VES5	4.55599	8.46011	1	8.44	2.3×10^{-3}	430.36	2.63	Moderate
VES6	4.55708	8.46057	5.08	13.6	6.1×10^{-4}	8322.64	3.92	Low
VES7	4.55522	8.45978	5.501	29.3	6.2×10^{-3}	887.49	2.95	Moderate
VES8	4.55681	8.46039	1.17	4.94	2.1×10^{-3}	535.93	2.73	Moderate
VES9	4.55637	8.46036	3.01	30	4.2×10^{-3}	714.03	2.85	Moderate
VES10	4.55561	8.46016	5.9	16.2	3.2×10^{-3}	184.43	2.27	Moderate
VES11	4.55647	8.46032	0.5	15.9	2.1×10^{-2}	22.93	1.36	High
VES12	4.55591	8.46032	6.02	5.09	1.2×10^{-2}	466.55	2.67	Moderate
VES13	4.55525	8.46143	10.38	13.9	2.6×10^{-2}	3986.16	3.60	Low
VES14	4.5544	8.46211	9.82	10	1.5×10^{-2}	649.67	2.81	Moderate
VES15	4.55674	8.46046	7.066	26.1	2.3×10^{-4}	30403.71	4.48	Extremely low
VES16	4.55503	8.46179	1.42	5.61	5.2×10^{-3}	272.43	2.44	Moderate

H cover = thickness of the protective layer, H aquifer = thickness of the aquifer, K = hydraulic conductivity of protective layer, K = hydraulic conductivity of protective layer, C = transverse resistance of protective layer
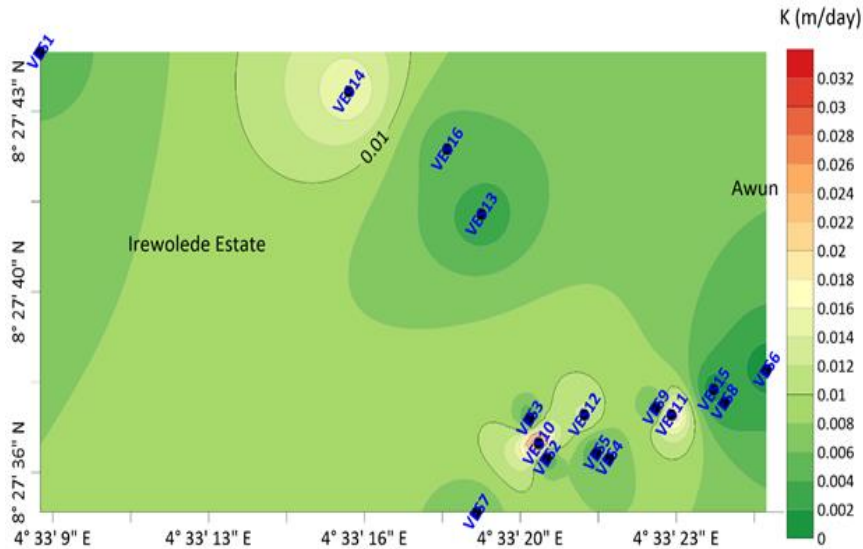
Figure 6. Contour map showing the variation of hydraulic conductivity.

4-4. AVI Rating

The proportion of AVI ratings in the study area is high (6.25%), low (25%), moderate (62.5%), and extremely high (6.25%). Figure 7 shows the spatial distribution of AVI across the study area. The majority of the area is rated moderate vulnerability, followed by low vulnerability. High and extremely low vulnerability occurs in small, isolated patches.

5. Conclusion

This study was conducted at Irewolede Estate in Ilorin, Kwara State, to evaluate the vulnerability of the weathered aquifer. The research employed vertical electrical sounding and IPI2WIN software to analyze the subsurface layers. The results showed that the area consists of 3 to 5geo-electric layers, including topsoil, sandy clay, laterites, weathered basement, and fresh basement. The weathered basement is the aquiferous layer, while the topsoil, sandy clay, and laterites serve as protective layers.

The study estimated hydraulic conductivity (K) to range from 2.3×10^{-4} to 3.2×10^{-2} mday^{-1} and hydraulic resistance from 22.93 to 30403.71 day^{-1}. The Aquifer Vulnerability Index (AVI) revealed that 62.5% of the area has moderate vulnerability, 25% low vulnerability, 6.25% high vulnerability, and 6.25% extremely high vulnerability. The spatial distribution shows that areas of moderate vulnerability are predominant, followed by low vulnerability areas, with high and extremely low vulnerability areas occurring in small, isolated patches. These findings can inform groundwater management and protection strategies.
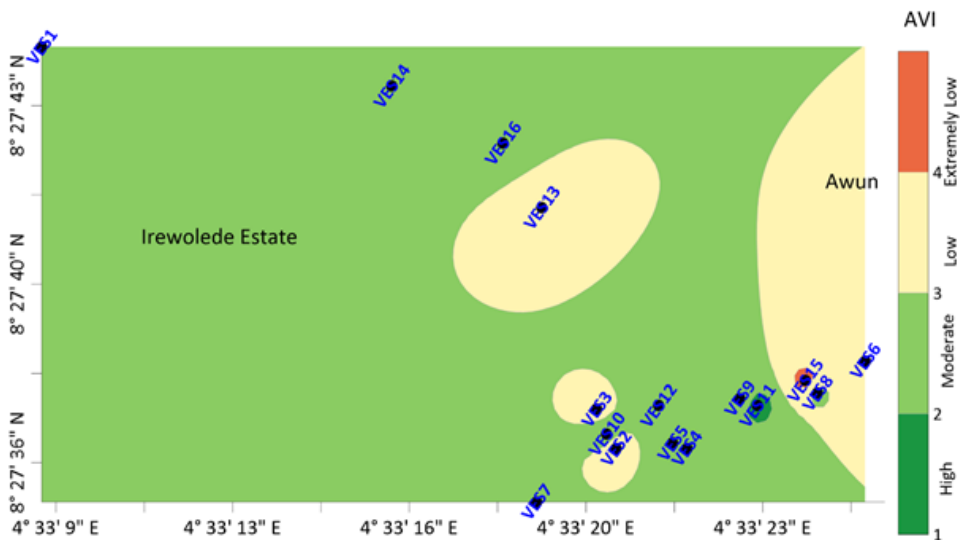

Figure 7. Protective capacity of the protective layer.

The study found that the poor water quality issues experienced by some residents are isolated cases, likely due to wells or boreholes drilled in areas with thin protective layers and high Aquifer Vulnerability Index (AVI) values. To prevent aquifer contamination, it is recommended that thorough geophysical and geotechnical studies be conducted before siting future landfills in the area. This approach will help identify safe locations and ensure the protection of the aquifer.

References

Amanambu, A. C., Obarein, O. A., Mossa, J., Li, L., Ayeni, S. S., Balogun, O., Oyebamiji, A., & Ochege, F. U. (2020). Groundwater system and climate change: Present status and future considerations. *Journal of Hydrology*, *589*, 125163. https://doi.org/10.1016/j.jhydrol.2020.125 163

Balogun, O. B. (2019). Tectonic and structural analysis of the Migmatite–Gneiss–Quartzite complex of Ilorin area from aeromagnetic data. *NRIAG Journal of Astronomy and Geophysics*, *8*(1), 22–33. https://doi.org/10.1080/20909977.2019.16 15795

Baweja, P., Kumar, S., & Kumar, G. (2020). Fertilizers and Pesticides: Their Impact on Soil Health and Environment. In B. Giri & A. Varma (Eds.), *Soil Health* (Vol. 59, pp. 265–285). Springer International Publishing. https://doi.org/10.1007/978-3-030-44364-1_15

Briffa, J., Sinagra, E., & Blundell, R. (2020). Heavy metal pollution in the environment and their toxicological effects on humans. *Heliyon*, *6*(9), e04691. https://doi.org/10.1016/j.heliyon.2020.e04 691

Ekanem, A. M. (2022). AVI- and GOD-based vulnerability assessment of aquifer units: A case study of parts of Akwa Ibom State, Southern Niger Delta, Nigeria. *Sustainable Water Resources Management*, *8*(1), 29. https://doi.org/10.1007/s40899-022-00628-x

Jain, H. (2023). Groundwater vulnerability and risk mitigation: A comprehensive review of the techniques and applications. *Groundwater for Sustainable Development*, *22*, 100968. https://doi.org/10.1016/j.gsd.2023.100968

Li, P., Karunanidhi, D., Subramani, T., & Srinivasamoorthy, K. (2021). Sources and Consequences of Groundwater Contamination. *Archives of Environmental Contamination and Toxicology*, *80*(1), 1–10. https://doi.org/10.1007/s00244-020-00805-z

Machiwal, D., Jha, M. K., Singh, V. P., & Mohan, C. (2018). Assessment and mapping of groundwater vulnerability to pollution: Current status and challenges. *Earth-Science Reviews*, *185*, 901–927. https://doi.org/10.1016/j.earscirev.2018.0 8.009

O, S. A., & A, A. A. (2018). Aquifer, Classification and Characterization. In M. S. Javaid & S. A. Khan (Eds.), *Aquifers—Matrix and Fluids*. InTech. https://doi.org/10.5772/intechopen.72692

Obiora, D. N., & Ibuot, J. C. (2020). Geophysical assessment of aquifer vulnerability and management: A case study of University of Nigeria, Nsukka, Enugu State. *Applied Water Science*, *10*(1), 29. https://doi.org/10.1007/s13201-019-1113-7

Olatunji, S., & Musa, A. (2014). Estimation of Aquifer Hydraulic Characteristics from Surface Geoelectrical Methods: Case Study of the Rima Basin, North Western Nigeria. *Arabian Journal for Science and Engineering*, *39*(7), 5475–5487. https://doi.org/10.1007/s13369-013-0846-0

Pointet, T. (2022). The United Nations World Water Development Report 2022 on groundwater, a synthesis. *LHB*, *108*(1), 2090867. https://doi.org/10.1080/27678490.2022.20 90867

Sethi, R., & Di Molfetta, A. (2019). Aquifer Vulnerability and Contamination Risk. In R. Sethi & A. Di Molfetta, *Groundwater Engineering* (pp. 137–159). Springer International Publishing. https://doi.org/10.1007/978-3-030-20516-4_7

Singh, P., Raj, A., & Yadav, B. (2022). Impacts of Agriculture-Based Contaminants on Groundwater Quality. In B. Yadav, M. P. Mohanty, A. Pandey, V. P. Singh, & R. D. Singh (Eds.), *Sustainability of Water Resources* (Vol. 116, pp. 249–261). Springer International Publishing. https://doi.org/10.1007/978-3-031-13467-8_16

Stempvoort, D. V., Ewert, L., & Wassenaar, L. (1993). Aquifer Vulnerability Index: A GIS - Compatible method for groundwater vulnerability mapping. *Canadian Water Resources Journal*, *18*(1), 25–37. https://doi.org/10.4296/cwrj1801025

Taghavi, N., Niven, R. K., Paull, D. J., & Kramer, M. (2022). Groundwater vulnerability assessment: A review including new statistical and hybrid methods. *Science of The Total Environment*, *822*, 153486. https://doi.org/10.1016/j.scitotenv.2022.153486

Tijani, M. N., Obini, N., & Inim, I. J. (2021). Estimation of aquifer hydraulic parameters and protective capacity in basement aquifer of south-western Nigeria using geophysical techniques. *Environmental Earth Sciences*, *80*(14), 466. https://doi.org/10.1007/s12665-021-09759-4

Udosen, N. I., Ekanem, A. M., & George, N. J. (2024). Geo-electrical prognosis of aquifer protectivity, corrosivity, and vulnerability via index-based models within a major coastal milieu. *Discover Geoscience*, *2*(1), 18. https://doi.org/10.1007/s44288-024-00020-6.